Study on the Land Surface Cover Dynamics of Built-up Areas and its Implication for Sustainable Urban Planning in Hawassa City, Ethiopia

Tikabo Gebreyesus Gerezgher (45tikabo@gmail.com)
Ethiopian Institute of Architecture, Building Construction and City Development, Addis Ababa University, Addis Ababa

Kumlachew Yeshitila Habtemariam
Ethiopian Institute of Architecture, Building Construction and City Development, Addis Ababa University, Addis Ababa

Aramde Fetene Mengistu
Ethiopian Institute of Architecture, Building Construction and City Development, Addis Ababa University, Addis Ababa

Cristina Herrero Jauregui
Complutense University of Madrid, Department of Biodiversity, Ecology, and Evolution, Madrid

Research Article

Keywords: Ground cover change, i-Tree canopy, Land surface temperature, Urbanization, Urban tree canopy

Posted Date: April 11th, 2022

DOI: https://doi.org/10.21203/rs.3.rs-1538652/v1

Abstract

Rapid and uncontrolled urbanization is one of the drivers responsible for land cover change dynamics in Ethiopia. In most of the cities and towns of Ethiopia, the proportion of different types of urban land surface cover and trends of change in each are unknown and thus hindering environmentally sustainable urban planning. This study describes different land surface cover types and their dynamics of change, and subsequent influence on the Land Surface Temperature of Hawassa city between 2011 and 2021. The i-Tree canopy and Landsat 5 (TM) and Landsat 8 (OLI) images were used for 2011 and 2021 to analyze the land surface cover and surface temperature change, respectively. The results show that bare soil is the dominant land surface cover type (23.4%), followed by tree canopy cover (21.4%), while impervious roads occupied the smallest land surface area cover (3.4%) along with water bodies (1%). In 10 years most of the land surface cover types increased positively, including tree covers by + 9.8%. The only exceptions were bare soil and herbaceous cover, which decreased drastically by -34.6% and − 2.8%, respectively. As a result of tree cover increment, the average and maximum Land Surface Temperature showed a declining trend between the two periods. This study shows that increasing tree cover in line with the expansion of urbanization is inversely correlated with the land surface temperature which implies that integrating green coverage along with the built-up area can reduce heatwave in the fast growing urban areas. Therefore, the Hawassa city administration should set tree cover targets to achieve the desired balance between green and grey infrastructure and enhance the climate resilience level of the study area.

1. Introduction

Land surface covers and land use types in urban areas are fine in texture and diversified in type compared to the land in the natural area. The ground surface of urban centers is the makeup of various cover classes, such as manmade and natural covers types (Nowak & Greenfield, 2020). Land surface cover of cities and towns is characterized by impervious layers, including buildings, roads, and parking lots, and other pervious surfaces – such as trees, grass, bare soil (Herold & Roberts; 2014; Nowak & Greenfield, 2020). According to the Natural Economy Northwest (2010), these cover types are categorized as grey and green elements. A ground surface with grass and grey cover is considered to be a potential site for new planting and non-plantable sites respectively (Jacobs et al., 2014). The grey covers are type of ground cover classes that comprises all constructed elements, while green components are all natural elements, including trees, shrubs, grass, and herb (Natural Economy Northwest, 2010). These land surface cover types in the urban environment are continually being changed due to rapid urbanization. A study by Berland (2012) that focused on the temporal land cover changes within 72 years caused by urbanization revealed that built-up areas increased dramatically from 19.15–66.58% at the expense of the natural elements. This anthropogenic induced phenomenon is one of the determinant factors that affects the sustainability of the cities and towns.

The human induced destruction of natural elements, such as vegetation causes energy fluxes between the land and the atmosphere (Lejeune et al., 2015). Urban expansion is one of the drivers that contribute to increasing the Land Surface Temperature (LST) of an area (Hereher, 2017). Consequently, urban centers are hotter than the surrounding rural areas by 1–6°C temperature difference (Ngie et al., 2014). This higher temperature in the urban area is due to the thermal properties of materials with higher conductive capacity and absorption of daytime temperature than materials of the rural area (Elsayed, 2012), a higher concentration of pollutants, and scarce vegetation cover is known as the urban heat island (UHI) effect (Rosenzweig et al., 2015). The raising of LST in the built-up environment is caused mainly by the land use cover change in general and land surface cover

change, in particular, is a result of the UHI (Jafari et al., 2017). The LST intensity within an urban area varies across different land uses with different ground surface coverage types. According to Chaka & Oda (2021), the highest mean temperature was recorded along roads, industrial zones, and waste disposal sites. Likewise, the lowest temperature was recorded in areas with the highest vegetation coverage, such as urban parks and lakeside greenery (Jafari et al., 2017; Chaka & Oda, 2021). However, the authors could not analyze the land/ground surface cover dynamics and correlate the results related to cover change dynamics with the trends of LST.

Baseline information on the trends of ground surface cover change is critically important to assess and understand sustainability trends of urban environments (Loveland et al., 2000) so that to respond to the impacts of climate change, including UHI effects. Likewise, available data on the proportion of tree canopy cover (TCC) and other pervious and impervious ground cover types is crucial to set a green cover target for cities to achieve within a certain time frame. A study by Doick et al. (2020) summarized environmentally sustainable urban centers should have TCC target goals of 20 to 40%. Using satellite images and remote sensing, several attempts have been made to quantify land use and land cover change in different urban centers of Ethiopia (Tadesse et al., 2001; Halefom et al., 2018; Mohamed & Worku,2019; Dessu et al., 2020), one of the cities with the fastest growing rate in the world. A study by Chaka & Oda (2021) concluded that the land use and cover change dynamics and vegetation conditions are some of the major factors that affect the LST variation across various land uses of Hawassa city, Ethiopia. However, neither of these studies has attempted to demonstrate the LST temporal changes caused by land surface cover change dynamics and TCC, pervious and impervious coverage proportion.

The use of coarse/low resolution images to estimate the ground covers of urban areas with fine coverage types could lead to misinterpretation of coverage types (Nowak & Greenfield, 2020). Thus, these authors rather suggest using a high resolution photointerpretation to quantify the existing coverage and detect the ground cover change in urban centers over time. The i-Tree canopy is a tool in which visual interpretation of land cover on aerial imagery can be conducted to analysis land surface cover type based on sample random points (Rogers & Jaluzot, 2015). Some i-Tree based researches, such as research by Mills et al., (2015) estimated ground surface cover and reported that areas dominated by structures, including commercial areas had the lowest TCC and higher grey cover, whereas Doick et al. (2017) highlighted that the temporal TCC change in different urban centers of Great Britain was both positive and negative.

Similar information for the urban centers of Ethiopia is lacking, so the current, historical and future TCC is unidentified. According to Ethiopia's Ministry of Urban Development and Housing [MUDH] (2015), 30% of the total land of every urban center in the country should be allocated for greenery purpose. However, a ground surface that can support the growth of vegetation and greenery development has not been identified and documented properly. This hinders urban planners, urban greenery managers, landscapers, and policymakers to build climate-resilient cities by achieving the proper green-grey balance of cities and towns in Ethiopia.

Therefore, this study aims at examining the environmental sustainability trends of Hawassa city in Ethiopia in the face of urbanization by evaluating the land surface cover change and its consequence on LST changes between 2011 and 2021. This research specifically focused on 1) determining the balance between grey and green coverage, 2) detecting the temporal dynamic of ground cover changes, and 3) demonstrating the effects of land surface cover change dynamics on LST between 2011 and 2021 in Hawassa city.

2. Methods And Materials

2.1. Study area

Hawassa city is seat of the recently established Sidama Regional State and South Nation Nationalities Governments and is located 275 km south of the capital, Addis Ababa city. Hawassa city administration comprises both plan and administration boundaries with a total of 157.2 km^2 area coverage. The plan boundary (excluding part of the city administration in the rural area) where the current study was conducted covers a total land surface of 51.98 km^2. Geographically, it is located in the central Rift valley of Ethiopia, extending from 6°55'00" to 7°06'00" latitude and 38°25'00" to 38°34'46" longitude (Fig. 1). Hawassa city has different topographic features with an elevation range between 1930 and 1680 meters above sea level (Hawassa City Administration, 2008).

The area has a mean annual precipitation of 973mm with mean annual 78.9 mm, and the highest intensity per unit time is in July and August with 29.3 and 34.8mm /day, respectively. The mean annual temperature ranges within 27.45 0C, 13.04 0C, and 20.25 0C during seasons with maximum, minimum, and mean temperatures, respectively. The monthly average maximum temperature of the area varies from 24.57 0C to 29.99 0C; the monthly average minimum temperature ranges from 10.36 0C to 14.58 0C, and the monthly average mean temperature varies from 19.32 0C to 21.57 0C (Hawassa City Administration, 2008).

Hawassa city is one of the urban centers in Ethiopia physically and economically growing at a rapid rate. According to the projection made in 2016 based on the census conducted in 2007, the current total population of city administration within the plan boundary is estimated as 319,023. The rapid horizontal expansion of the city that was noticed within the last 20 years has contributed to the conversion of significant area of natural land into a built-up area. For instance, the agricultural area at the periphery has been converted into a settlement, transportation infrastructure, and other facilities. This expansion of the city beyond its boundary is due to population growth, emerging economic activities, and national and local urban land policies (World Bank, 2016).

Institutional forests, amenity green spaces and private gardens, neighborhood green spaces, street trees, public parks, green spaces around industrial and commercial areas, green belts, and lakeside green spaces are some of the common green infrastructure (GI) types in the study area. Most of these GI types are found in the inner city under the intensive management of the city administration except the green belt. The green belt is dominated by natural vegetation and native species at the ridge called Alamura. This GI type belongs to the city administration but is not part of the inner city greenery practices (Fig. 1). In this study, analysis was performed considering the land surface cover of the green belt as part of the inner city greenery practices and excluding it from the analysis to explicitly understand the contribution of manmade greenery to increase TCC.

2.2. Method

2.2.1. Sampling Design and Sample size

The TCC and other ground surface cover classes of the study area were simulated using i-Tree canopy software. The i-Tree canopy is one of the components of the i-Tree tool developed by the United Sstates Forest Service in 2006. It is a free access web-based tool (Doick et al., 2017), that can produce quantified and statistically provides valid values for various land surface cover types (Givens, 2019).

The sampling procedure followed four major steps: 1) definition of the study area boundary by importing boundary shapefile of the built-up part of Hawassa city into the i-Tree canopy, 2) predefinition of the land surface cover types to be surveyed (Table 1), and 3) classification of each random point overlapped on the aerial image that shows the land surface cover types categorized as ‘Tree/shrub’ or ‘Non-Tree’. The defined area for this study includes the urbanized part of the city (hereafter called plan boundary administration, Fig. 1).

The land surface cover types predefined in this study are presented in Table 1. Pervious surface classes (bare soil/ground, pervious roads, herbs, grass, and other permeable surface types) along with impervious surfaces (tar/asphalted roads, buildings, cement, and ceramic cover surfaces) were grouped into the 'Non-Tree' category. Furthermore, the tree and shrubs were classified under the 'Tree' category

Table 1
Predefined ground surface cover classes, number of sample points randomly laid over different cover types, and the estimated area occupied by each ground surface cover class

Cover Class	Description	Category	Points (n)	Area (ha)
Grass/herbaceous	Maintained and unmaintained grass and herbaceous ground cover including crops	Non-Tree	68	733
Buildings	Buildings with steeled roofs and other structures	Non-Tree	98	1057
Other impervious	Large solid rock outcrops, cement, ceramic, man-hole covers, utility boxes, headstones	Non-Tree	34	367
Impervious road	Road constructed from asphalt/tar, cement, ceramic and impervious materials	Non-Tree	17	183
Other pervious	Organic/inorganic mulch, gravel, brick, flagstone, compacted soil, etc.	Non-Tree	22	237
Pervious roads	Roads and other walkways constructed from permeable and semi-permeable materials, such as cobblestones, gravel, compacted soil, and the likes	Non-Tree	32	345
Soil/bare ground	Exposed soil including naturally occurring sand.	Non-Tree	117	1262
Tree/Shrub	Any woody trees and shrubs	Tree	107	1154
Water	Wetland, artificial ponds, and lakes	Non-Tree	5	54

The land surface cover of the study area was quantified using a random point sampling procedure. Sample points (displayed as yellow crosses in Fig. 2) were randomly distributed by the i-Tree software onto the most recent Google Map image (2021), and the materials that covered the ground were classified by interpreting the coverage types (Givens, 2019) within the geographically defined boundary.

A total of 500 random sample points were repeatedly added and classified as Tree or Non-Tree (Table 1). The upper limit for the sample points for each of the predefined cover class types was determined based on the Standard Errors (SE = ± 2) of cover classes that display amidst the i-Tree canopy survey (Doick et al., 2020), calculated as.

$$SE = \frac{\sqrt{\mathrm{p}(1-\mathrm{p})}}{\mathrm{N}} (1)$$

Where p is estimated as n/N, n number of points that hit a particular ground surface class and N is the total number of random points generated for all cover class types distributed across the study area.

Sampling data can be affected by the skills and knowledge of the land cover interpreter, image resolution, shaded ground by building, and other difficulties to identify the correct cover types at some points (Parmehr et al., 2016). About 2.2% (11 points) of the random points overlapped on the 2021 Google Map image i-Tree canopy could not be identified due to those challenges. Thus, a ground truth survey was conducted to overcome it by exporting the coordinates of those unidentified points from the image and located them using geographical positioning system (GPS). However, the ground surface cover reclassified in the 2011 Google Earth image was not complicated as the area was more open and easily identified from the image.

2.2.2. Historical land surface cover coverage analysis (2011)

To assess the coverage trends of the study area in the last 10 years, the 2021 Google Earth image was switched back to the historical image of October 2011. The same sample random points generated in the 2021 image were transferred to the 2011 image (Fig. 3). Then, sample points were reclassified using the same ground surface classes (Givens, 2019).

2.2.3. Land Surface Temperature Estimation

Landsat 5 thermal band 6 and Landsat 8 thermal band 10 with 30 m spatial resolutions for 2011 and 2021 respectively were used to quantify the Land Surface Temperature (LST) of the study area. The Landsat 5 thermal band 6 was used to estimate both variables in 2011, while Landsat 8 thermal band 10 for 2021. These Landsat Images of both periods were downloaded from the United State Geological Survey (USGS) and pre-processed.

The thermal band 10 (thermal infrared band) of Landsat 8 was used to retrieve the LST by converting the Digital number (DNs) to radiances. A set of equations was applied and the two variables were calculated using a raster image in ArcGIS. The equations (2–7 for Landsat 8 thermal band 10) employed in this study are described below based on the algorithm developed by Avdan & Jovanovska (2016). Converting the digital number into radiance is the first step that was computed as:

$$TOA = M_L * Q_{cal} + A_{L-O_i} (2)$$

Where TOA (Watts/(m^2× srad × μm)) is the top atmospheric radiance, M_L represents the band-specific multiplicative rescaling factor, Q_{cal} is the Band 10 image, A_L is the band-specific additive rescaling factor, and O_i is the correction for Band 10.

Further, the Brightness Temperature (BT) in degree Celsius (°C) was calculated as:

$$BT = \frac{K_2}{\ln[(K_{1\,/\,TOA)} + 1]} - 273.15 (3)$$

Where $K1$ and $K2$ stand for the band-specific thermal conversion constants from the metadata file

The NDVI values were calculated using the Landsat visible and near-infrared Bands (see Eq. 10) to determine the vegetation proportion (Pv) since it is an important factor that affects the land surface emissivity (ε) (Avdan & Jovanovska, 2016).

$$\mathrm{Pv} = \frac{NDVI - NDVI_{MIN}}{NDVI_{MAX} - NDVI_{MIN}} (4)$$

Thereafter, the surface emissivity is calculated using the vegetation proportion as:

$$\epsilon = 0.004 * \mathrm{Pv} + 0.986 (5)$$

Where P_v is the proportion of vegetation computed from the NDVI. Finally, the LST of the study area during 2021 was estimated as:

$$LST = \frac{\mathrm{BT}}{\{1 + \left[\left(\frac{\lambda \mathrm{BT}}{\rho}\right) \ln \epsilon_{\lambda}\right]\}} (6)$$

Where Ts is the LST in Celsius (∘C), λ is the wavelength of emitted radiance.

The Landsat 5 thermal band 6 image, launched in 1984 and was operational until 2013, was used to estimate the LST and NDVI values of the study area in 2011 (Yang et al., 2015). Similarly, the raw image in the form of Digital Numbers (DNs) was converted into radiance as:

$$\mathrm{L}_{\lambda} = \left(\frac{LMAX_{\lambda} - LMIN_{\lambda}}{QCALMAX - QCALMIN}\right) x (QCAL - QCALMIN) + LMIN_{\lambda} (7)$$

Where L_{λ} is Spectral Radiance; $LMIN_{\lambda}$is the spectral radiance that is scaled to QCALMIN (DNs = 0); $LMAX_{\lambda}$ is the spectral radiance that is scaled to QCALMAX (DNs = 255); $QCALMIN$ is the minimum quantized calibrated pixel value (corresponding to$LMIN_{\lambda}$) in DN; $QCALMAX$ = the maximum quantized calibrated pixel value (corresponding to$LMAX_{\lambda}$) in DN, and $QCAL$ = the quantized calibrated pixel value in DNs.

The spectral radiance is converted to brightness temperature (BT) taking into account the emissivity is constant (Yang et al., 2015).

$$\mathrm{T} = \frac{\mathrm{K2}}{\ln(\mathrm{K1}/\mathrm{L}_{\lambda} + 1)} (8)$$

Where T is effective at satellite temperature in Kelvin

K1 and K2 are calibrated constant 1 and 2 (W/m2*sr*μm), respectively

L_{λ} is spectral radiance in (W/m2*sr*μm)

The NDVI value was quantified for both periods to comprehend the trends of vegetation condition and its effect on the heat island of the study area. Thus, the NDVI values for 2011 and 2021 are estimated from Landsat 5 thermal band 6 and Landsat 8 thermal band 10 respectively computed according to the following equation.

$$NDVI_{landsat5} = \frac{NIR(Band4) - R(Band3)}{NIR(Ban4) + R(Band3)} (9)$$

$$NDVI_{landsat8} = \frac{NIR(Band5) - R(Band4)}{NIR(Ban5) + R(Band4)} (10)$$

Where NIR represents the near-infrared band (Band 5) and R represents the red band (Band 4 and Band 3). NDVI value ranges from − 1 to 1. When the NDVI value closes to − 1 or 0, it indicates bare land or water body, whereas when the value approaches 1, vegetation vigor/dense vegetation.

2.2.5. Statistical analysis

The nature of the data derived from the i-Tree software makes it impossible to correlate with the raster image derived LST. Thus, the TCC was substituted by the NDVI that was quantified from a satellite image to statistically test the effect of vegetation cover change on LST. A Pearson regression analysis was performed to test the correlation between the NDVI derived from raster images and LST results. The raster dataset of Landsat 8 and Landsat 5 for LST was estimated according to equations 6 and 8, and equations 9 and 10 for NDVI were overlaid in the ArcGIS and converted into tabular form. Spatial random points within the boundary of the study area with NDVI and LST values were generated from the two raster images. Thereafter, a Pearson regression analysis was carried out using SPSS software.

3. Results

3.1. Current Ground surface Cover (2021)

According to the land surface cover analysis of this study for 2021, the highest cover proportions were observed on ground surface cover types identified as bare land, TCC category (‘Tree/shrub’), and impervious building with 1262 ha 23.4 ± 1.89%, 1154 ha (21.4 ± 1.83%), and 1057 ha (19.60 ± 1.78%) respectively (Fig. 4). The relative coverage of impervious roads accounted for 183 ha (3.4 ± 0.81%), which was the least coverage proportion next to the water body with a total of 54 ha (1 ± 0.45%). Moreover, herbaceous plant vegetation cover had a coverage share of 733 ha (13.60 ± 1.53%) and land surface cover types under the category of impervious other contributed to 367 ha 6.80 ± 1.13% (Table 2).

A road constructed from cobblestone, compacted soil, gravel, and the like that were considered as pervious road in this study was estimated at 345 ha (6.40 ± 1.09%), while all pervious ground covers (pervious other) that cover the land surface in different land uses other than roads shared coverage of 237 ha (4.40 ± 0.92%).

Land surface cover analysis was performed by excluding and including a green belt (GB) at the periphery to understand the manmade green space contribution to raising the overall greenery of the city. The average tree coverage of Hawassa city by excluding the GB from the analysis decreased from 21.4–19.5%, while all impervious surfaces (building, impervious roads, and other impervious) merged raised from 28.80–34.3% when the GB was excluded from the analysis. The permeable surface coverage decreased in the second scenario, whereas building coverage alone increased (Table 2).

Table 2
Summary of ground cover classes considering GB as part of the inner-city green spaces and excluding from the inner city

Coverage category	Cover classes	Including GB		Excluding GB	
Grey		**Cover (ha)**	**Cover (%)**	**Cover (ha)**	**Cover (%)**
	Buildings/roof	**1057 ± 96**	**19.60 ± 1.78**	**1148 ± 109**	**21.75 ± 2.06**
	Other impervious	**367 ± 61**	**6.80 ± 1.13**	**488 ± 76**	**9.25 ± 1.45**
	Impervious road	**183 ± 44**	**3.40 ± 0.81**	**172 ± 47**	**3.25 ± 0.89**
Green	**Tree/Shrub**	**1154 ± 99**	**21.40 ± 1.83**	**1029 ± 105**	**19.50 ± 1.98**
	Grass/herbaceous	**733 ± 83**	**13.60 ± 1.53**	**647 ± 87**	**12.25 ± 1.64**
Bare land	**Other pervious**	**582 ± 108**	**10.80 ± 1.01**	**343 ± 65**	**6.50 ± 1.23**
	Soil/Bare ground	**1262 ± 102**	**23.40 ± 1.89**	**1385 ± 116**	**26.25 ± 2.20**
Waterbody	Water	54 ± 24	1.00 ± 0.45	66 ± 30	1.25 ± 0.56

By merging these ground surface classes, grey cover which encompasses buildings, impervious roads, pervious roads, and other impervious and pervious surfaces together accounted for 40.6% of the study, whereas barren land accounted for 23.4%. The green elements (trees, shrubs, grass, and herbs) collectively in the green spaces under the intensive maintenance of the city administration and the naturally existing green belt contributed to 36% of the total land.

3.2. Temporal dynamics of ground surface cover

According to the results presented in Fig. 5, significant hectares of land surface cover of the urbanized part of the city were changed within the ten-year time interval. A positive cover change between 2011 and 2021 was noted in most cover types except herbaceous and bare land (soil) classes that were decreased from 16.4–13.6% (-2.8%) and from 58–23.4% (-34.6%), respectively. Notably, the highest positive increment was observed in TCC increased from 11.6–21.4%, next to impervious buildings that raised from 19.6–21.75%.

The impervious road which was 0.8 in 2011 increased to 3.4% in 2021, while pervious roads increased from 4.4 to 6.4%. Likewise, the coverage type categorized as 'impervious other' increased from 2.8–6.8%, while no significant change was noted in the water body coverage (Table 3).

Table 3
Temporal and spatial land surface cover change of Hawassa city between 2011 and 2021

Cover Class	Year 2011					Year 2021					
	Cover (ha)	± SE (ha)	Cover (%)	± SE (%)	Points	Cover (ha)	± SE (ha)	Cover (%)	± SE (%)	Points	Change (%)
Herbaceous	884	89	16.4	1.66	82	733	83	13.6	1.53	68	-2.8
Buildings	194	45	3.6	0.83	18	1057	96	19.6	1.78	98	16
Imperv. other	151	40	2.8	0.74	14	367	61	6.8	1.13	34	4
Imperv. road	43	22	0.8	0.4	4	183	44	3.4	0.81	17	2.6
Pervious other	86	30	1.6	0.57	8	237	49	4.4	0.92	22	2.8
Pervious roads	237	49	4.4	0.92	22	345	59	6.4	1.09	32	2
Bare land	3127	119	58	2.21	290	1262	102	23.4	1.89	117	-34.6
Tree	625	77	11.6	1.43	58	1154	99	21.4	1.83	107	9.8
Water	43	22	0.8	0.4	4	54	24	1	0.45	5	0.2

The grey surface cover that includes buildings, impervious and pervious roads, and a ground cover categorized as ‘other impervious’ together positively changed from 13.2–40.6% (+ 27.4%), whereas all green elements together increased from 28.8–36% (+ 7.2%). However, the permeability of the urban area decreased as a result of the falling of all pervious surfaces (previous road, bar land/exposed soil, and ‘other pervious’) from 61.7–36% (-34.6) (Fig. 6).

3.3. Land Surface Temperature Changes Trends of the study area

The LST of the study area ranged from 18.38–35.65°C in 2011 and 18.97–33.48°C in 2021 (Fig. 7). Results revealed that the minimum, average, and maximum LST of the study area in 2011 were 18.38, 27.71, and 35.65°C, respectively. The maximum and average LST decreased to 33.48 and 26.04°C, while the minimum temperature slightly increased by 0.6°C during 2021.

Likewise, LST spatial variation was also observed in the study area in both periods. The highest LST with values 27–30°C was recorded at the city center (the oldest part of the city) in both years, while LST beyond 30°C was noted in industrial zones, residential areas, and central business district areas of the city (Fig. 7). The areas in the eastern part of the city being developed towards the fringe, the green belt with natural forest, and the Lakeside in the Western part had less LST (below 23°C).

3.4. Relationship between LST and NDVI

The vegetation coverage pattern of Hawassa city based on the estimated NDVI values in 2011 and 2021 is presented in Fig. 8. The NDVI values recorded in the study area were between − 0.29 to 0.61 in 2011 and − 0.06 to 0.51 in 2021. A relatively highest average NDVI value of 0.23 was recorded in 2021, whereas 0.17 in 2011. The minimum NDVI values in 2011 and 2021 were − 0.29 and − 0.06 respectively. However, the maximum NDVI value (0.61) in 2011 was slightly greater than the values in 2021 (0.51) regardless of the area coverage.

According to the NDVI value reclassified as very low density (< 0.1), low (0.1 to 0.2), medium (0.2 to 0.3), and high (0.3 to 0.6), a spatial variation was observed in value distributions across the study area. The total area with a high NDVI value area cover decreased from 11% in 2011 to 7% in 2021, while the very low NDVI density increased by 2% in 2021. Low and medium values also increased from 38% in 2011 to 39% and from 29–30% in 2021, respectively. This implies that areas with low NDVI values (Fig. 8) had the highest LST recorded during both periods.

The correlation between vegetation cover and temperature in both years was statistically significant (p-value = 0.00) with the correlation measure (R^2) values of 0.472 and 0.592 for 2011 and for 2021 respectively (Fig. 9). Subsequently, it was assured that the maximum annual temperatures of the study area were recorded in the areas with the lowest NDVI values.

4. Discussion

As far as urban centers are economic hubs, urbanization is an inevitable phenomenon throughout the world. Thus, the environmental damages due to urbanization in Ethiopia could be alleviated by letting the urban development has to be based on the master plan and structural plan. The central arguments explicitly explored in this paper are the positive contributions of urbanization on the urban tree cover and built structures over the expenses of the low ground cover (grass, bare soil, and other herbs). Subsequently, expanding cities based on such proper urban planning would help to lower the heat island of the human-dominated landscapes.

Studies on the urban land surface cover and temporal changes based on sample points using i-Tree software have been commonly conducted in many US cities (e.g., Nowak & Greenfield, 2012; Nowak & Greenfield, 2020), some European urban centers (e.g., Mills et al., 2015; Doick et al., 2017; Doick et al., 2020), and few Asian cities (e.g., Atasoy, 2020). To our knowledge, no study has been conducted so far following similar approaches to explore the trends of urban land surface cover changes in cities and towns in Africa. Thus, this study has reported pioneer findings on the land surface cover dynamics and environmental implications of the cities and towns in Ethiopia. As far as urban centers are similarly characterized in terms of ground cover type dynamics, the results of this study were compared to the findings of similar studies conducted in Europe, the US, Asia, and other regions of the world.

Attempts were made to analyze the current and change of the urban fabrics from which the urban land is covered. This helps to understand the impacts of urbanization on land surface cover compositions and change dynamics. Subsequently, it can assist to rethink the proper balancing of the grey, green, and blue cover classes of the built environment. Thus, understanding the current green-grey cover proportion of the built environment can enhance the sustainability of cities and towns (Banzhaf et al., 2018; Corbane et al., 2020).

Materials that cover every land parcel of the study area were estimated based on the 500 random sample points of the i-Tree software that were distributed across the study area. Indeed, studies on urban land use and cover

change analysis have been increasingly using spatial scale satellite images that could affect the quality data presentation to study the ground cover types of urban areas with fine scale. A study by Parmehr et al. (2016) compared land cover quantified using i-Tree software based on 1000 random points and remotely sensed data shows that the variation between the two results was 1%. Thus, approaching this research using a different procedure would provide a similar output.

4.1. Current ground surface cover (2021)

The results of this study showed that a considerable proportion of the land surface of the city is bare soil (about 1262 ha or 23.4%). This implies that the city has potential areas for tree planting to raise the current TCC (21.4%) to the desired coverage level that urban centers around the world are set to achieve. The trees, shrubs, grass/herb, and other green elements, which collectively contributed to covering a total land surface of 36%, can help to curb the expansion of grey components that currently shared 40.5% coverage. A result of previous research by Mills et al. (2015) reported a range of green coverage from 30.4 to 30.74%, including the natural forest coverage of the green belt. The current TCC (tree/shrub canopy cover = 21.4%) of the study area fulfilled the minimum TCC standard that sustainable cities and towns need to have. According to Doick et al., (2017), healthy and livable cities should set a target to achieve at least 20% tree canopy cover. However, if excluding the natural forest coverage of the green belt surrounding the inner part of the built part of the city, the TCC of the study area is slightly below this standard (19.5%). Thus, the green belt tree cover has contributed about 2% to raise the total TCC of the study area. One of the previous researches by Atasoy (2020) demonstrated the remarkable roles of natural vegetation cover surrounding a city that increases the overall canopy cover and cover per capita. Many cities have such natural and semi-natural types of green belts mainly protected and maintained to reduce the grey dominance over the green regardless of their inaccessibility to provide other services.

4.2. Land surface cover and Temperature changes

Human dominated landscapes, such as the expansion of settlements and other infrastructures due to urbanization can also contribute towards the increment of TCC. A positive temporal TCC change was observed in this study. The annual increment of impervious and tree coverage types shown in this study is in line with the study by Nowak (1993) in Oakland that urban tree cover increased as the intensity of urbanization increased. On the contrary, a study by Berland (2012) in Minnesota reported that urbanization was the cause for the annual TCC losses estimated at 9.6%. Likewise, a study by Nowak & Greenfield (2020) that attempts to explore the land surface coverage dynamics of urban centers around the globe reported that the tree coverage of urban centers in Africa declined between 2012 and 2017. The same authors reported that the average tree canopy coverage of cities and towns in Africa was about 20%, which is similar to the current TCC (19.4%) excluding the green belt of Hawassa city. A study by Gashu & Gebre-egziabher (2018) analyzed the land use and land cover change of Hawassa city using satellite images and showed that vegetation cover decreased by 14%. However, the authors reported that the grey coverage of the city increased by 24% from 1973 to 2015, which is almost equivalent to the pervious coverage of the current study (24.6%). Nevertheless, this research was focused on the temporal changes of the general land cover changes in terms of use regardless of the ground surface cover on which the current study focused. In general, the role of urbanization on the losses and increasing rate of land surface cover depend on the land use history of an area.

Although urban tree coverage can be increased in line with urbanization, the expansion of built-up areas exuberates the destruction of natural elements, including vegetation cover and soil. The results of this study

show that a large area of pervious land coverage of the study area, such as herbaceous/grass and bare land/soil declined, which could be due to the expansion of the grey coverage (e.g., building, road, and other impervious types). The gaining of grey surface cover (+ 24%) is over the expenses of the coverage loss of grass (-2.8%) and bare soil (-34.6%) covers. This implies that plantable spaces of the city have been converted into grey cover to expand other infrastructures. This result is in line with the study by Nowak & Green (2018), who reported the impervious surface cover was gained from the loss of trees, grass, and herbaceous coverage. Thus, total canopy cover from large trees and shrubs could temporally be increased in cities and towns, whereas the losses of lower layer ground covers (herbs, soil) decreased as the rate of urbanization intensified.

Understanding the land use history of areas around cities and towns is critically important to comprehend the positive or negative impacts of urbanization on land surface cover. The expansion of built areas over the previously forested area can play a great role in declining the green coverage of an urban area (Nowak & Green, 2018). In this study, however, tree canopy coverage increased as the rate of urbanization increased. Likewise, the percentage of areas with high and low/very low NDVI values increased and decreased respectively within the stated timeframe. This could be because an important part of Hawassa city has been expanded into the previously undeveloped agricultural area (barren land) which had no tree cover until 2011.

There are driving factors that affect the decline or gaining of green coverage in the urban center around the world. For instance, tree coverage could be raised due to the increment in tree planting initiatives and activities around the human-dominated landscapes, such as institutional areas, commercial and residential areas (Nowak & Greenfield, 2020). Moreover, town planning, changes in vegetation preference of community, and management activities (Doick et al., 2020) can contribute to the gaining of TCC in the face of rapid urbanization. The first structural plan of Hawassa city was prepared in 1951 with a total land of 120 ha of which most of the land was allocated for housing purposes (Federal Urban Planning Institute, 2006). The updated five-year structural plans (2007–2021) revealed that neighborhood green spaces, closed natural parks, and public recreational green infrastructures are important elements of the land use types of the city. Thus, the increment in the green area coverage per capita from 0.52m² in 1998 to 2.0m² by the year 2011 is one of the indicators that the structural plan is an important tool to raise the green coverage of the city. Subsequently, vacant spaces with few patches of vegetation and dominated by bare land in 2011 have been turned into closed parks and other recreational areas. For instance, the presently closed public park with enacted natural forest called Millennium Park was a vacant space with scatter native tree species in 2011; and significant green spaces established along the lakeside as a buffer of the Hawassa Lake could significantly contribute to increasing the TCC. It was clearly stated in the structural plan that the strategies employed to attain the required green coverage were encouraging environmental advocators, private sectors, and mobilizing the community to participate in tree planting and green area developments.

These positive roles of urbanization towards TCC could contribute to lowering the land surface temperature of the study area. This study shows that the LST of the study area decreased by -1.84°C between 2011 and 2021, while the green coverage in general and tree canopy cover in particular raised by + 7.2% and + 9.8%, respectively. The increment of tree canopy cover following the settlement expansion towards the natural area has contributed to lowering the LST. Gill et al., (2007) also reported that raising the urban green spaces by 10% in the most built part of a city contributes to decreasing the maximum surface temperature by 2.2°C. The authors also pointed out that this amount of green spaces addition in a high and low emission scenario decreases LST by 2.4°C and 2.5°C, respectively. The same authors also reported that the removal of 10% green space coverage in high and

low emission scenarios could raise the LST by 7°C and 8.2°C, respectively. Similarly, the current study confirmed that increasing trees, shrubs, grass, and herb, collectively green coverage by 9.8% or raising the TCC alone by 7.2% contributes to decreasing the maximum and average LST by -2.17°C and − 1.67°C, respectively.

It was not possible to carry out a correlation analysis between the LST derived from raster images and TCC estimated using the i-Tree canopy software due to the nature of the data from this software. Thus, the TCC was replaced by the NDVI to test the effects of vegetation cover on LST. The NDVI values are usually between − 1 and + 1; however, areas with different types of ground cover type could have various levels of NDVI values. In the case of the current study, the average NDVI value in 2021 was higher (0.23) than in 2011 with 0.17. About 17% (880 ha) of the total area of the city in 2021 had the maximum NDVI value of 0.5, while small land size (490 ha) of the city had the highest vegetation coverage with the same NDVI value in 2011. The urban area is dynamic and the ground cover type is subjected to frequent temporal and spatial changes. Thus, the NDVI values vary across the study area. According to Ya'Acob et al. (2014), water bodies, rocky/barren land, greenery, and dense forest have less than zero (negative), -0.1 to 0.1 (value close to zero), 0.1–0.4 zero (low positive), and up to + 1 NDVI values, respectively. According to the NDVI values of the current study, more than 20% of the city in 2011 had sites with no vegetation coverage (NDVI = < 0.1), whereas this proportion decreased to 18% in 2021. There are green spaces and some patches of the urban forest before 2011 and still exist in Hawassa city where the highest NDVI values in both periods could be recorded. According to Warkaye et al. (2018), the highest NDVI with 0.5–0.7 values were reported in the green belt, urban green spaces, and river banks, while the lowest values with 0.31–0.5 in the closed urban park of Addis Ababa city. However, this study was focused on selected parks only, while the current study was conducted on the entire city of Hawassa. Areas with 0.2 to 0.4 NDVI were classified as medium vegetation and more than 0.4 value was considered as areas with high vegetation cover (Nandargi & Kamble, 2017). Regarding the NDVI spatial pattern shown in Fig. 8, the highest land surface area of the city with 0.3–0.5 NDVI values in 2021, whereas the major part of the city (66.7%) in 2011was with less than or equal to 0.20 NDVI value due to the less coverage of green spaces.

According to the result of the statistical analysis with R^2 = 0.472 for 2011 and 0.592 for 2011, about 47% and 59% of the LST in 2011 and 2021 respectively decreased due to the vegetation coverage in the study. In addition to the vegetation components, the water bodies could also play important roles to reduce the LST. Adulkongkaew et al. (2020) suggested the conversion of the built area into a landscape with 20% tree canopy, 30% of blue components (water bodies), and 40% of shrubs and other green elements is effective to reduce the LST of urban areas. Thus, it is critically important to take into consideration the proportion of land cover composition at the urban planning and implementation stages to reduce the impacts of heat island effects.

The Normalized Difference Vegetation Index and tree canopy cover can be used as indicators of LST trends. The highest temperature at the center of the city and other built areas where the lowest NDVI values records indicates that the heat island effect is due to the low vegetation cover and thermal properties of the ground cover materials. This study confirmed that LST decreased as both TCC and NDVI increased within the 10 year time. Thus, the two variables can be used interchangeably to examine the effects of vegetation cover on LST trends. The statistical analysis result of the study revealed that vegetation cover and the heat island effect have a reverse correlation. This study is in line with the research by Warkaye et al. (2018) conducted in Addis Ababa city who concludes that the NDVI value of different urban parks increased as the LST of the study area decreased from 1985 to 2015. Thus, increasing annual urban tree coverage in urban centers is the effective strategy of urban heat island effective adaptation strategy.

5. Conclusion

The findings of the study from the combination of the i-Tree canopy and Landsat images with the proper thermal band on the land surface cover change dynamics and the influences of urban tree cover on the LST would help to understand the heat island effect trends of the study area. The result of the study from the i-Tree canopy analysis showed that the major cover types, such as green and grey, increased from 2011 to 2021 at the expense of the pervious surface layers. This finding indicated that the positive increment of these cover types could be gained from the dramatically declined bare land and herbaceous cover types. The agricultural area with no trees, but a considerable area of open/bare land at the periphery of Hawassa city during 2011 has been turned into settlement and other infrastructure so that green spaces have been established following development activities. Thus, this study ensured urbanization can play a great role to add not only grey elements but also man-made green spaces at the expense of the natural environment, such as grass and soil.

The result from the Landsat 5 and Landsat 8 thermal band 6 and 10 analyses respectively revealed that the Land Surface Temperature of the study area declined between 2011 and 2021. It is most often expected that the LST has to intensify in the face of urban expansion due to its adverse impacts on the natural elements and thermal property of ground cover types in the built-up area. However, this study revealed that increasing tree cover was in line with urbanization as radiance surface temperature was decreased. Thus, green infrastructure elements in general and urban trees, in particular, are effective strategies to develop climate resilient cities. Thus, the raster image derived NDVI result was in line with the i-Tree canopy derived TCC increment in Hawassa city. Moreover, as both TCC and NDVI temporally and spatially increased, the LST decreased within the last 10 years. This study shows that both TCC and NDVI can be used as indicators of the general trends of heat island effect, but further study is required to measure the TCC and NDVI level of effect on the heat island effect of cities.

Understanding the dynamicity and trends of urban land use cover change in general and land surface cover in particular helps to comprehend the composition of land surface coverage of cities and towns and sustainability trends. The findings of this research will provide new insights into the sustainable environmental management roles of green infrastructure, increasing the understanding of planners and policymakers on the effectiveness of increasing TCC to lower LST, and community appreciation regarding the roles of urban trees in alleviating urban heatwave. As a result, the proper integration of green infrastructure as one of the major elements of urban planning to improve the sustainability of the cities and towns would come into being. The stakeholders at different levels can rethink the strategies of balancing and proper green, grey cover, and other pervious covers ratio in the urban centers. Thus, looking for pathways in the process of urban planning that contribute to enhancing the TCC to reach the minimum recommended green coverage would be easily achieved once the current and cover change are comprehended.

The livability and climate resilience of the study area would be improved well than what is at present through proper urban green infrastructure planning. TCC and other green elements can be increased by turning unnecessary structures in different parts of the city being overwhelmed by grey elements into green and blue cover types. Likewise, converting sites with excessive grass, herb, and bare land covers into tree planting can increase the TCC in the built-up area and improve the potential of the city to respond to the effect of the heat island. The other important thing that planners and policymakers should give due attention to is the proper incorporation of adequate tree cover at each planning stage so that to have the proper green, grey and other cover

type proportions. This study can be used as base map information about the current and historical coverage can be used to inform the urban planning actors regarding the present and future sustainability trends of the city.

Declarations

Acknowledgments

We, the authors, would like to thank the ***NORAD*** project office based under the management of ***Hawassa University, and Addis Ababa University*** for their contributions to partially financing this research work. Our especially gratitude goes to the **Professor Cristina Herrero Jauregui** for hosting and provision of necessary facilities for the corresponding author during the data analysis and report writing.

Funding

Partial financial support was received from Hawassa University and Addis Ababa University to accomplish this work.

Competing interests,

The authors have no competing interests to declare that are relevant to the content of this article.

Ethics approval

Since this study is an observational study, the authors confirmed that no ethical approval is required.

References

1. Adulkongkaew, T., Satapanajaru, T., Charoenhirunyingyos, S., & Singhirunnusorn, W. (2020). Effect of land cover composition and building configuration on land surface temperature in an urban-sprawl city, case study in Bangkok Metropolitan Area, Thailand. Heliyon, 6(8), e04485. https://doi.org/10.1016/j.heliyon.2020.e04485
2. Atasoy, M. (2020). Characterizing the spatial structure of urban tree cover (UTC) and impervious surface cover (ISC) density using remotely sensed data in Osmaniye, Turkey.
3. Avdan, U., & Jovanovska, G. (2016). Algorithm for automated mapping of the land surface temperature using Landsat 8 satellite data. Journal of Sensors, 2016, 8. https://doi.org/10.1155/2016/1480307
4. Berland, A. (2012). Long-term urbanization effects on tree canopy cover along an urban-rural gradient. Urban Ecosystems, 15(3), 721–738. https://doi.org/10.1007/s11252-012-0224-9
5. Chaka, D. S., & Oda, T. K. (2021). Understanding land surface temperature on rift areas to examine the spatial variation of urban heat island: the case of Hawassa, southern Ethiopia. GeoJournal, 86(2), 993–1014. https://doi.org/10.1007/s10708-019-10110-5
6. Corbane, C., Martino, P., Panagiotis, P., Aneta, F. J., Michele, M., Sergio, F., Marcello, S., Daniele, E., Gustavo, N., Thomas, K., Corbane, C., Martino, P., Panagiotis, P., Aneta, F. J., Michele, M., Sergio, F., Marcello, S., Daniele, E., & Gustavo, N. (2020). The grey-green divide: multi-temporal analysis of greenness across 10, 000 urban centres derived from the Global Human Settlement Layer (GHSL). International Journal of Digital Earth ISSN:, 8947(1), 101–118. https://doi.org/10.1080/17538947.2018.1530311

7. Crown. (2007). The Urban Environment. ROYAL COMMISSION ON ENVIRONMENTAL POLLUTION.
8. Dessu, T., Korecha, D., Hunde, D., & Worku, A. (2020). Long-Term Land Use Land Cover Change in Urban Centers of Southwest Ethiopia From a Climate Change Perspective. Frontiers in Climate, 2(December), 1–23. https://doi.org/10.3389/fclim.2020.577169
9. Doick, K. J., Buckland, A., & Clarke, T. K. (2020). Historic urban tree canopy cover of Great Britain. Forests, 11(10), 1–16. https://doi.org/10.3390/f11101049
10. Doick, K. J., Davies, H. J., Moss, J., Coventry, R., Handley, P., Vazmonteiro, M., Rogers, K., & Simpkin, P. (2017). The Canopy Cover of England's Towns and Cities: baselining and setting targets to improve human health and well-being. Trees People and the Built Environment 3, 1–27. www.urbantreecover.org
11. Elsayed, I. S. M. (2012). Mitigation of the urban heat island of the city of Kuala Lumpur, Malaysia. Middle East Journal of Scientific Research, 11(11), 1602–1613. https://doi.org/10.5829/idosi.mejsr.2012.11.11.1590
12. Federal Urban Planning Institute. (2006). Integrated Development Plan Report for Hawassa City. Ministry of Works and Urban Development Federal Urban Planning Institute, Addis Ababa, Ethiopia.
13. Gashu, K., & Gebre-egziabher, T. (2018). Spatiotemporal trends of urban land use / land cover and green infrastructure change in two Ethiopian cities: Bahir Dar and Hawassa. Environmental Systems Research, 8(7), 1–15. https://doi.org/10.1186/s40068-018-0111-3
14. Gill, S. E., Handley, J. F., Ennos, A. R., & Pauleit, S. (2007). Adapting cities for climate change: The role of the green infrastructure. Built Environment, 115–133(1), 115–133. https://doi.org/10.2148/benv.33.1.115
15. Givens, E. (2019). Crystal River Canopy Analysis: 2005–2015. Legacy Arborist Services, Florida.
16. Halefom, A., Teshome, A., Sisay, E., & Ahmad, I. (2018). Dynamics of Land Use and Land Cover Change Using Remote Sensing and GIS: A Case Study of Debre Tabor Town, South Gondar, Ethiopia. Journal of Geographic Information System, 10(02), 165–174. https://doi.org/10.4236/jgis.2018.102008
17. Hereher, M. E. (2017). Effect of land use/cover change on land surface temperatures - The Nile Delta, Egypt. Journal of African Earth Sciences, 126, 75–83. https://doi.org/10.1016/j.jafrearsci.2016.11.027
18. Herold, M., & Roberts, D. A. (2014). The Spectral Dimension in Urban Remote Sensing. In F. D. van der Meer & A. Marçal (Eds.), Remote Sensing and Digital Image Processing (pp. 47–66). Springer Science + Business Media B.V. 2010. London New York.
19. Jacobs, B., Mikhailovich, N., & Delaney, C. (2014). Benchmarking Australia's Urban Tree Canopy: An i-Tree Assessment, prepared for Horticulture Australia Limited by the Institute for Sustainable Futures, University of Technology Sydney.
20. Jafari, E., Soltanifard, H., Aliabadi, K., & Karachi, H. (2017). Assessment of the Effect of Neyshabur Green Spatial Configuration on the Temperature of Land Surface and Heat Islands. Open Journal of Ecology, 07(09), 554–567. https://doi.org/10.4236/oje.2017.79037
21. Lejeune, Q., Davin, E. L., Guillod, B. P., & Seneviratne, S. I. (2015). Influence of Amazonian deforestation on the future evolution of regional surface fluxes, circulation, surface temperature and precipitation. Climate Dynamics, 44(9–10), 2769–2786. https://doi.org/10.1007/s00382-014-2203-8
22. Loveland, T. R., Reed, B. C., Ohlen, D. O., Brown, J. F., Zhu, Z., Yang, L., & Merchant, J. W. (2000). Development of a global land cover characteristics database and IGBP DISCover from 1 km AVHRR data. International Journal of Remote Sensing, 21(6–7), 1303–1330. https://doi.org/10.1080/014311600210191

23. Mills, G., Anjos, M., Brennan, M., Williams, J., McAleavey, C., & Ningal, T. (2015). The green 'signature' of Irish cities: An examination of the ecosystem services provided by trees using i-Tree canopy software. Irish Geography, 48(2), 62–77. https://doi.org/10.2014/igj.v48i2.625
24. Ministry of Urban Development and Housing [MUDH]. (2015). Ethiopia national urban green infrastructure standard. Addis Ababa, Ethiopia.
25. Mohamed, A., & Worku, H. (2019). Quantification of the land use/land cover dynamics and the degree of urban growth goodness for sustainable urban land use planning in Addis Ababa and the surrounding Oromia special zone. Journal of Urban Management, 8(1), 145–158. https://doi.org/10.1016/j.jum.2018.11.002
26. Nandargi, S. S., & Kamble, A. S. (2017). Temporal and Spatial Analysis of Rainfall and Associated Normalized Difference Vegetation Index (NDVI) over the Pune District, India. Focus on Sciences, 3(4), 1–6. https://doi.org/10.21859/focsci-03041452
27. Natural Economy Northwest. (2010). "Putting the green in the grey": Creating sustainable grey infrastructure (Vol. 3).
28. Ngie, A., Abutaleb, K., Ahmed, F., Darwish, A., & Ahmed, M. (2014). Assessment of urban heat island using satellite remotely sensed imagery: A review. South African Geographical Journal, 96(2), 198–214. https://doi.org/10.1080/03736245.2014.924864
29. Nowak, D. J. (1993). Historical vegetation change in Oakland and its implications for urban forest management. Journal of Arboriculture, 19(5), 313–319.
30. Nowak, David J, & Green, E. J. (2018). Declining urban and community tree cover in the United States. Urban Forestry & Urban Greening, 32, 32–55. https://doi.org/10.1016/j.ufug.2018.03.006
31. Nowak, David J, & Greenfield, E. J. (2012). Tree and impervious cover change in U. S. cities. Urban Forestry & Urban Greening, 11, 21–30. https://doi.org/10.1016/j.ufug.2011.11.005
32. Nowak, David J, & Greenfield, E. J. (2020). The increase of impervious cover and decrease of tree cover within urban areas globally (2012–2017). Urban Forestry & Urban Greening, 49(January). https://doi.org/10.1016/j.ufug.2020.126638
33. Parmehr, E. G., Amati, M., Taylor, E. J., & Livesley, S. J. (2016). Estimation of urban tree canopy cover using random point sampling and remote sensing methods. Urban Forestry and Urban Greening, 20, 160–171. https://doi.org/10.1016/j.ufug.2016.08.011
34. Rogers, K., & Jaluzot, A. (2015). Oxford i-Tree Canopy Cover Assessment 2015. Treeconomics.
35. Tadesse, W., Tsegaye, T. D., & Coleman, T. L. (2001). Land use/cover change detection of the city of Addis Ababa, Ethiopia using remote sensing and geographic information system technology. International Geoscience and Remote Sensing Symposium (IGARSS), 1(C), 462–464. https://doi.org/10.1109/igarss.2001.976190
36. UCCRN. (2015). Climate Change and Cities: Second Assessment Report of the Urban Climate Change Research Network ARC3.2. Center for Climate Systems Research, Earth Institute, Columbia University.
37. Warkaye, S., Suryabhagavan, K.., & Satishkumar, B. (2018). Urban Green Areas to Mitigate Urban Heat Island Effect: The Case of Addis Ababa, Ethiopia. International Journal of Ecology and Environmental Sciences, 44(4), 353–367.
38. Ya'Acob, N., Azize, A. B. M., Mahmon, N. A., Yusof, A. L., Azmi, N. F., & Mustafa, N. (2014). Temporal forest change detection and forest health assessment using remote sensing. IOP Conference Series: Earth and

Environmental Science, 19(1). https://doi.org/10.1088/1755-1315/19/1/012017

39. Yang, R., Guan, P., Cai, K., Xiao, W., Si, X., & Zhaofeng, Z. (2015). J estr. Journal of Engineering Science and Technology, 8(3), 14–20.

Figures

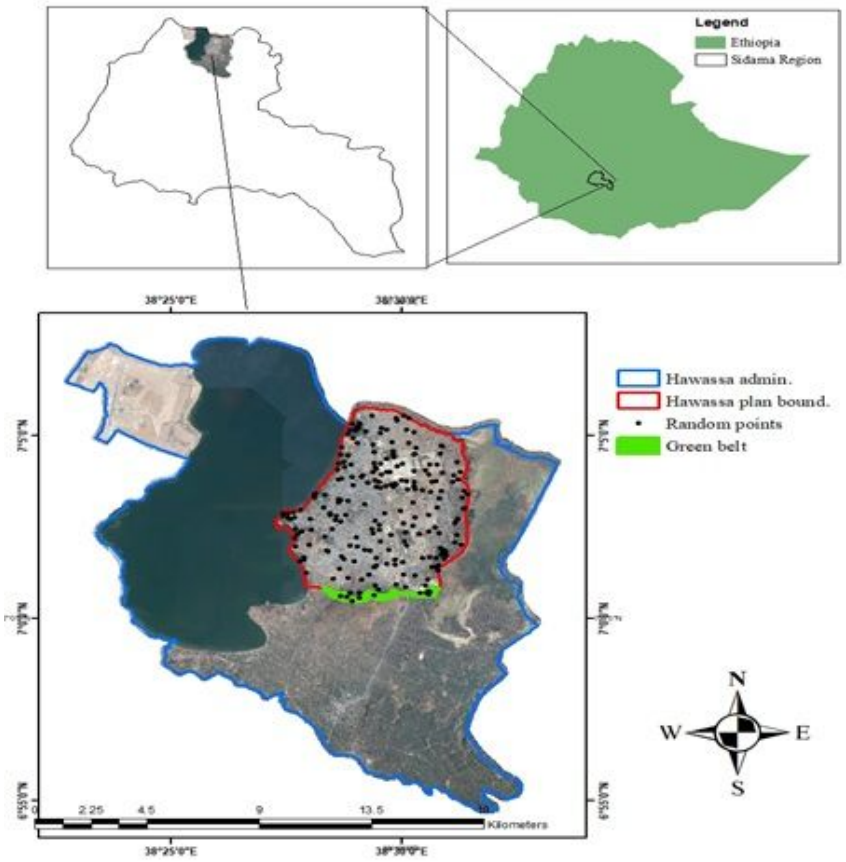

Figure 1

Geographical Location of the study area, Hawassa city administration

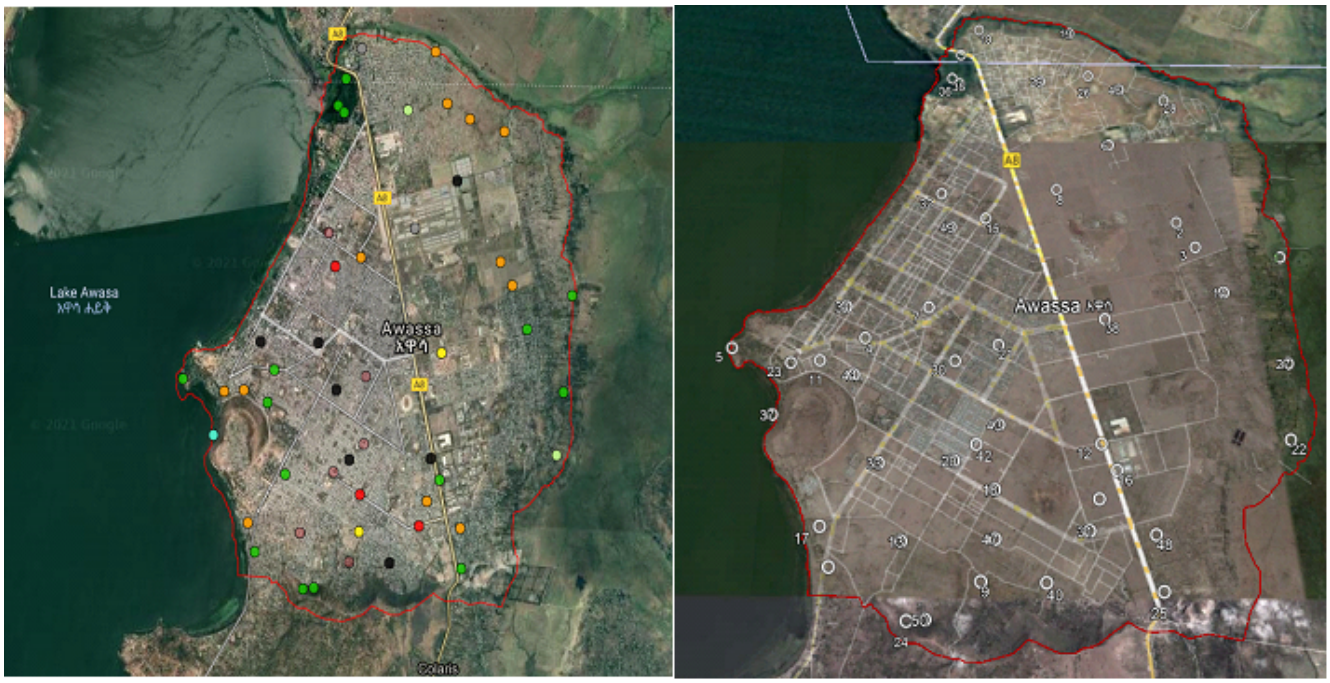

Figure 2

Sample points distributed on the aerial image 2021 of the i-Tree canopy tool exported (left) and random points transferred from i-Tree project and overlaid on the image Google Erath 2011 (right).

Figure 3

Land/ground surface cover types (where a = impervious building; b = impervious asphalted road; c = barren soil; d = tree/shrub) of the study area classified in the i-Tree software based on the yellow crosshairs overlaid in the aerial Google Map image 2021 (Source: screenshot from the image in the i-Tree canopy software)

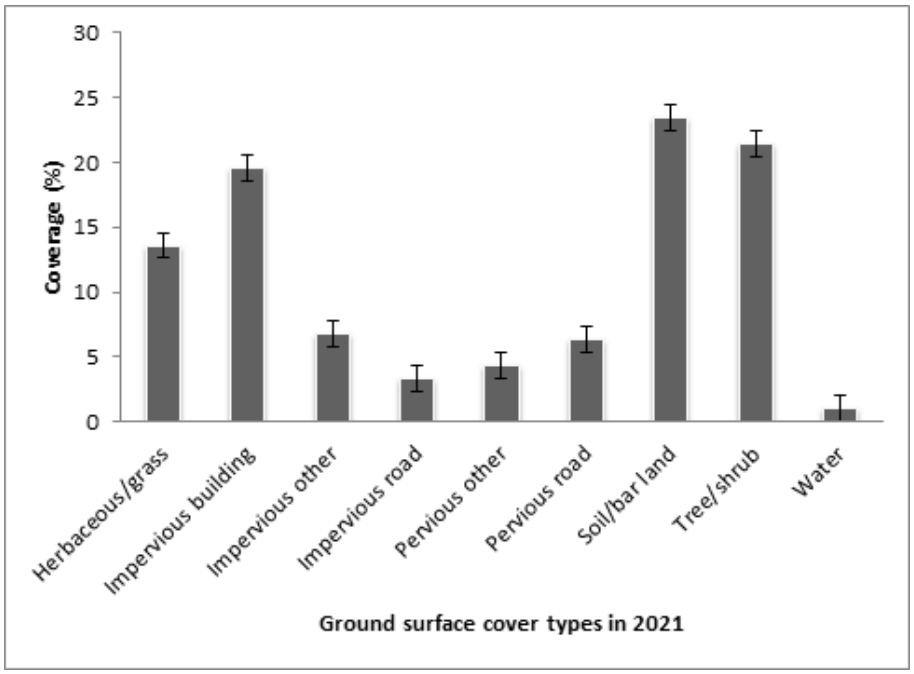

Figure 4

Percentage of ground surface covers classes in Hawassa city for 2021

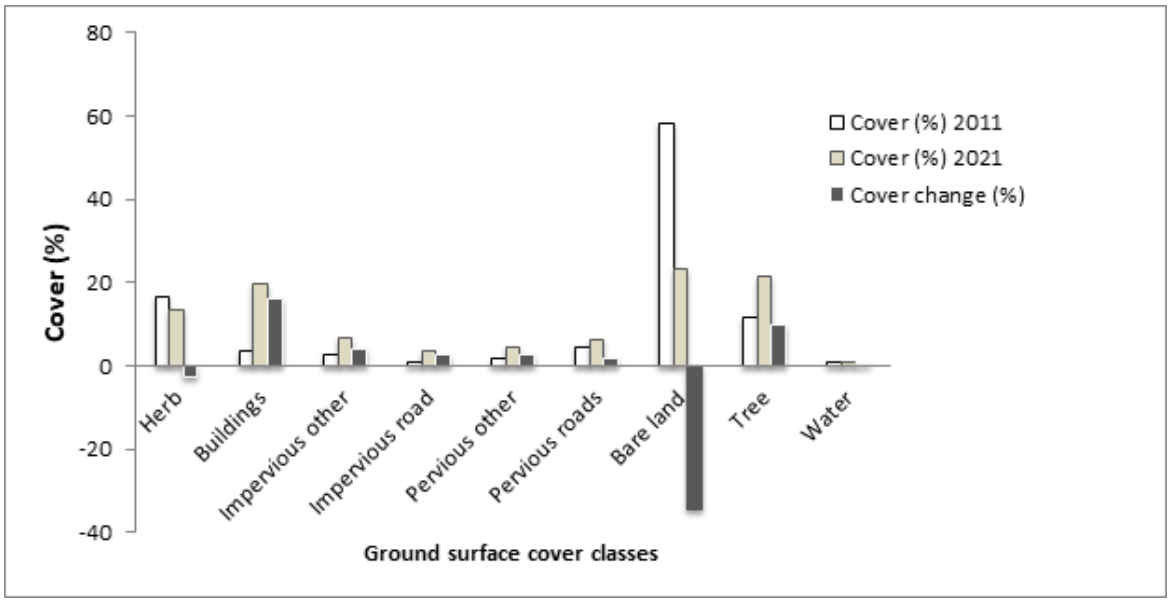

Figure 5

Ground surface cover change between 2011 and 2021 in the study area

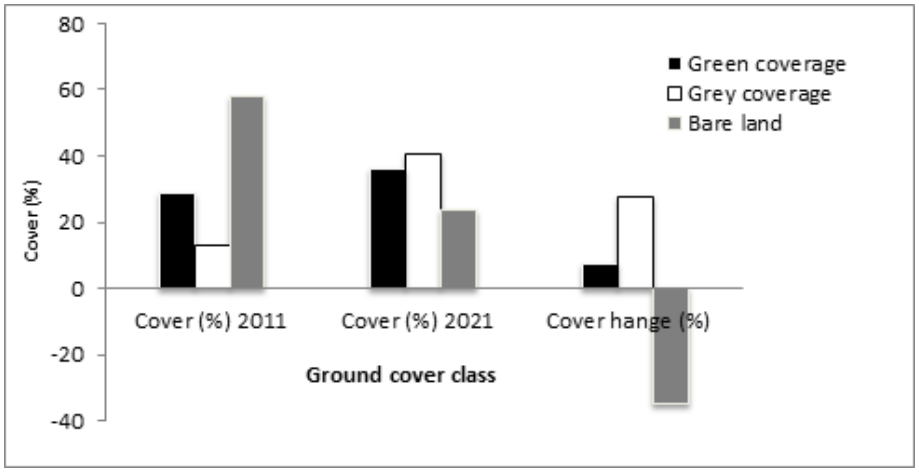

Figure 6

Change trends of grey, green and bare land/soil coverage over the last ten years

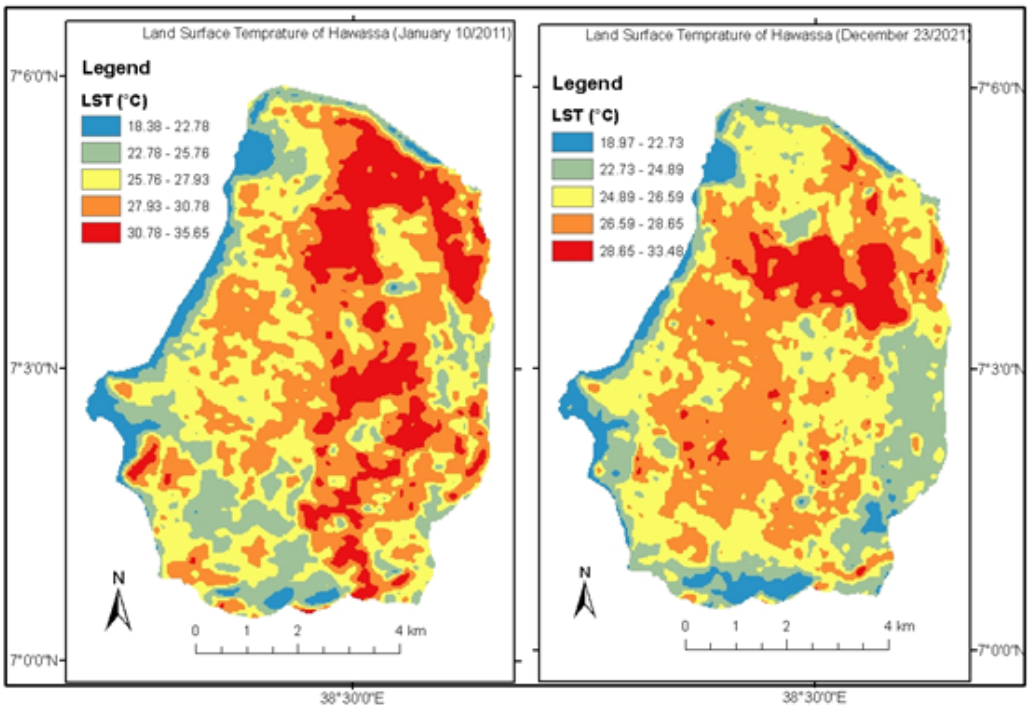

Figure 7

Spatial Land Surface Temperature variation across the study area between 2011 and 2021

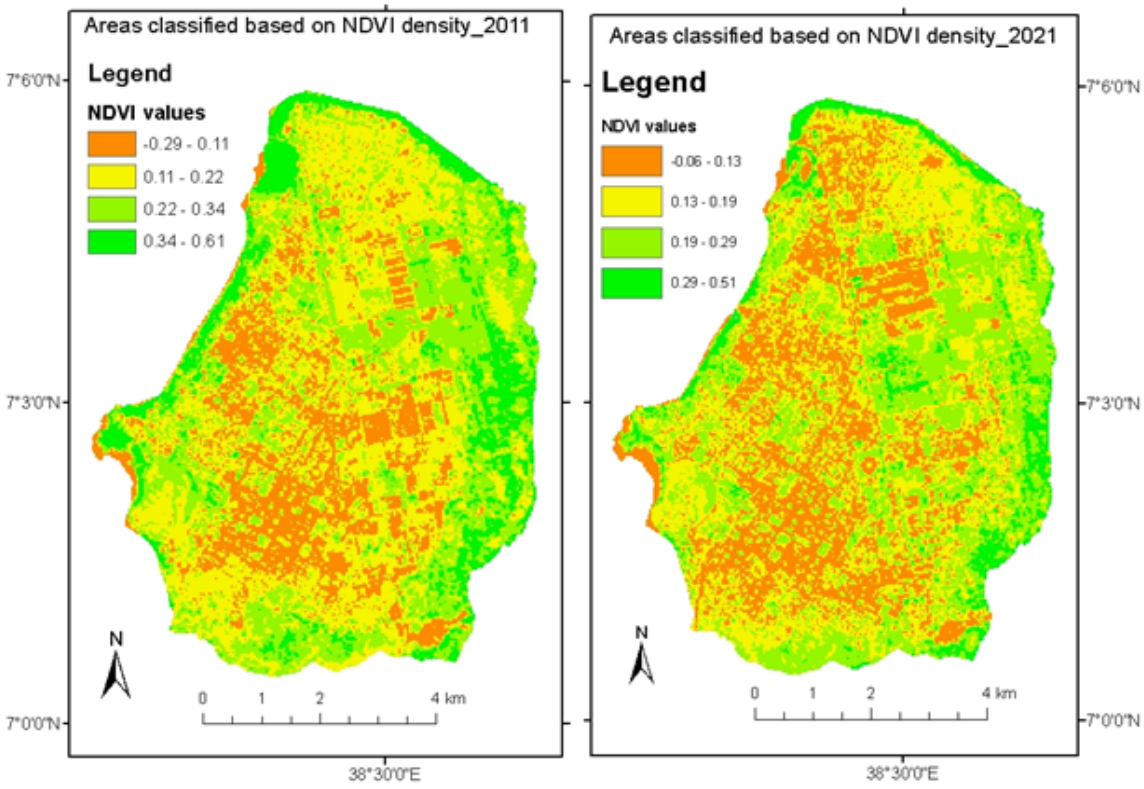

Figure 8

Normalized Difference Vegetation Index of the study area in 2011 and 2021

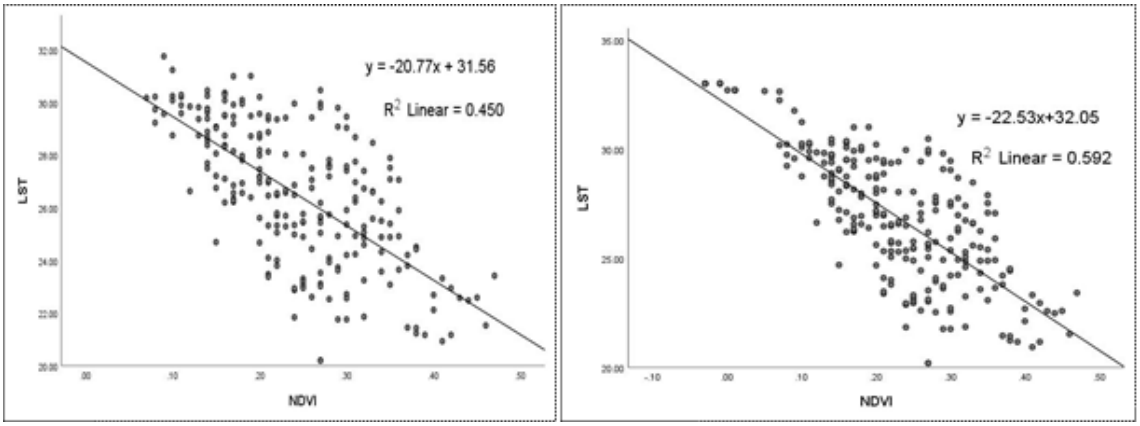

Figure 9

Relationship between LST and NDVI of the study area between 2011 and 2021